Journal of Engineering Research

Volume 7 | Issue 1 Article 17

2023

Experimental Investigation of the Thermal-hydraulic Performance of Conically Coiled Tubes using Al2O3/Water Nanofluid

Mohamed Abdelghany

Journal of Engineering Research (ERJ)
Vol. 7 – No. 1, 2023
©Tanta University, Faculty of Engineering
ISSN: 2356-9441 https://erjeng.journals.ekb.eg/ e ISSN: 2735-4873

Experimental Investigation of the Thermal-hydraulic Performance of Conically Coiled Tubes using Al_2O_3/Water Nanofluid

Mohamed T. Abdelghany [1*], M.A. Sharafeldin[2], O.E. Abdellatif [2] and Samir M. Elshamy[1]

[1] High Institute of Engineering, October 6 City, Egypt.
[2] Mechanical Engineering Department, Faculty of Engineering at shoubra, Benha University, Egypt
[*] Corresponding Author emails: mohamed.tawfik@csi.edu.eg, mohamed5558@yahoo.com

***Abstract*- The thermal-hydraulic performance of conically coiled tubes (*CCT*s) was investigated experimentally under constant heat flux boundary conditions in this study. The effect of several factors, such as the flow Dean number, coil torsion, and varied nanoparticle weight concentrations, on the flow's heat transfer coefficient and pressure drop was studied. Thermo-hydraulic performance was studied at 0.3%, 0.6%, and 0.9% volume concentrations (φ) of *Al_2O_3/water* nanofluid, a Dean number (*De*) of 1148–2983, and coil torsions (λ) ranging from 0.02 to 0.052. Results indicated that the heat transfer rates (*HTR*s) of *CCT*s increased when the coil torsion was decreased. According to the findings, the average heat transfer coefficient (h_{avg}) rises as *De* increases, while friction factor (*f*) tends to decrease. The average increase in h_{avg} is 32% at lower *De* values and 26% at higher *De* values as the nanofluid concentration increased from 0.3% to 0.9%. The thermal performance factor (*TPF*) improved when λ lowered from 0.052 to 0.02.**

***Keyword*: Nanofluid; Conical coiled tubes; Thermal performance Factor; Coil torsion; Heat transfer.**

I. INTRODUCTION

Numerous scientific studies have demonstrated that heat transfer rates (*HTR*s) in coiled tubes surpass those of straight tubes. Due to its compact design and efficient *HTR*, this type of coil is able to deliver a substantial heat transfer area in a little space. In the current era, adding nanoparticles to base fluids can improve heat transfer capability. These nanotechnology-based fluids, termed as nanofluids, have outstanding properties such as high thermal conductivity. Today, nanofluids are used to improve thermal performance in a wide variety of applications [1–6]. Recent research has proven that the use of nanofluids and coiled tubes concurrently may considerably increase the *HTR* [7–9].

Heyhat et al. [10] examined the effect of nanofluids and *CCT* geometrical variables on pressure drop and heat transfer. With studies performed under laminar conditions, various SiO_2/water concentrations were utilised. As geometric variables, different cone angles and coil pitches were utilised. According to the data, increasing the coil pitch enhances the *HTR*. Moreover, cone angle variation enhances heat transfer more effectively than coil pitch variation. Sheeba et al. [11] studied the experimental and numerical heat transfer properties of a *CCT* heat exchanger. According to their observations, the inner Nusselt number was substantially affected by the inner and annulus Dean number. Moreover, according to their results, the employment of a *CCT* heat exchanger as opposed to an *HCT* type may result in an increase in the overall heat transfer coefficient.

Mansouri and Zamzamian [12] investigated experimentally the *HTR* and pressure drop properties of Al_2O_3/water nanofluid within a horizontally helically coiled tube (*HCT*). Results demonstrated that the h increased by 6.4%, 19.0%, and 23.7%, respectively, for heat fluxes of 2283 and 4975 W/m^2 at a 1 wt% concentration of *Al_2O_3/water* nanofluid compared to pure water. Hasan and Bhuiyan [13] investigated the thermal performance and the entropy generation of a *HCT* heat exchanger with different coil revolutions utilizing a 5% concentration of *Al_2O_3/water* nanofluid. Results demonstrated that when coil revolutions increase, the total *HTR* and friction factor increase. Maximum entropy generation increased by 19.5% when the coil revolution was varied but the rib profile remained unchanged.

Sundar and Shaik [14] studied experimentally the *TPF* at varied volume fraction of water and *EG* mixture based *ND* nanofluids flow in a shell and *HCT* heat exchanger. According to observations, at a Reynolds number of 2702 and a volume fraction of 1%, *h* and *Nu* are enhanced by 36.05 and 27.47 %, respectively, and the *TPF* is enhanced by 1.2094 compared to the base fluid. Hasan et al. [15] studied numerically the heat transfer performance of an *HCT* heat exchanger using various nanofluids, taking into account diverse head-ribbed geometries with varied coil revolutions. The *HTR* was increased by 20% to 80% using a 2-rib head geometry and by 17% to 66% using a 30-turn coil. It has been determined that *Al_2O_3* has the maximum *HTR*, whereas SiO_2 has the lowest.

Kia et al. [16] conducted a computational and experimental investigation of the *HTR* and pressure drop characteristics of *Al_2O_3* and *SiO_2/Base oil* nanofluid flow in a *HCT* subject to uniform heat fluxes. The results demonstrated that using nanofluid in place of the base fluid boosted the heat transfer factor and pressure drop. The greatest *HTR* is associated with *Al_2O_3* and SiO_2 nanofluid volume concentrations of 0.5%, which are 41.4% and 27.3% greater than base oil, respectively. Güngor et al. [17] investigated the thermal performance of a new shell

DOI: 10.21608/ERJENG.2023.192940.1152

Journal of Engineering Research (ERJ)
Vol. 7 – No. 1, 2023
©Tanta University, Faculty of Engineering
ISSN: 2356-9441 https://erjeng.journals.ekb.eg/ e ISSN: 2735-4873

and *HCT* heat exchanger design with integrated rings and discs both numerically and experimentally. The results showed a 22.1% average rise in the overall coefficient of heat transfer for a 3 l/min hot fluid flow rate as well as a 19.6% average growth for a 4 l/min.

Fuxi et al. [18] investigated the effects of employing hybrid nanofluids in a shell and *HCT* heat exchanger. One of the effective variables in boosting the rate of heat transfer is the impact of increasing the *Re*. Thus, at a pitch of 20 mm and a volume fraction of 4%, a 66.7% rise in *Nu* was seen when the Re number increased from 10,000 to 20,000. Tuncer et al. [19] utilized single and hybrid type nanofluids to investigate the thermal performance of a shell and *HCT* heat exchanger with and without fins. It was discovered that the effect of utilizing TiO_2*/water* single and *CuO–*TiO_2*/water* nanofluids at high *Re* is comparatively greater than at lower *Re*. Also, It was discovered that using a single-type TiO_2*/water* nanofluid on the coil side of shell and *HCT* heat exchanger with and without fins resulted in an average 9.2% and 14% improvement in the coefficient of heat transfer, respectively.

Kumar and Chandrasekar [20] investigated the *HTR* and friction factor of *MWCNT* nanofluids in a double *HCT* heat exchanger. It is believed that *MWCNT*/water nanofluids resulted in a greater convective heat transfer than water. It is also believed that heat transfer rises with increasing *MWCNT*/water nanofluid volume fraction. At a 0.6% volume concentration of *MWCNT*/water nanofluids at a flow rate of 140 L/ h and a Dean number of 1400, the greatest convective heat transfer of 35% was observed. Al-Abbas et al. [21] conducted experimental research and exergy analyses on shell and *HCT* heat exchangers for free convection heat transfer. It has been demonstrated that exergy efficiency increases linearly with increasing *De* and decreasing volume flow rates of cold water. Moreover, as the diameter of the coil increases, the pressure drop decreases noticeably.

Shafiq et al. [22] investigated numerically the thermal performance enhancement of shell and *HCT* heat exchangers utilizing *MWCNTs*/water nanofluid. The findings indicate that the *Nu* of the fluid flowing through the coil improved as the Re of the coil and nanofluid volume concentration rose. When a 0.5% volume concentration of *MWCNT*/water nanofluid was employed at a coil Re of 15,000, the maximum improvement in *Nu*, i.e., 31.5%, and the highest-pressure decrease, 47.35 %, were found under the same situations. Khalil et al. [40] studied experimentally the impact of placing coil wire in the shell side of a double-pipe heat exchanger on pressure drop and heat transfer. As comparison to the smooth pipe, the heat transfer coefficient rose up to 1.59 while the pressure drop increased 10 times. Findings also shown that the increase in heat gain is far greater than the reduction in pumping power.

Khosravi-Bizhaem et al. [41] studied experimentally the *HTR* and the entropy generation for nanofluid flow through *HCT*s. The findings demonstrated that *Ag* nanoparticles increase thermal conductivity and *h* by 8 to 25%, *MWCNT*/water increases the *HTR* by up to 10%, whilst *GO* nanoplates reduce the *HTR*. Recent experimental and computational investigations into heat transfer in coiled tubes are represented in Table 1.

Regardless of the fact that substantial study has been performed on nanofluids and *HTC*s independently, only a few studies have been completed on the case of merging the *CCT*s and nanofluids approaches, and more research is required. Experimentally investigating the thermal-hydraulic performance of Al_2O_3*/water* nanofluid flow within *CCT*s with a uniform heat flux. All experiments were conducted using a broad range of Dean number (*De)*. The authors look at how the nanofluid concentration, *De*, and coil torsion affect heat transfer and pressure drop along the *CCT*s.

Table 1. A summary of the recent literature on coiled tubes

Reference	Year	Approach	Geometry	Working Fluid
Alimoradi et al. [31]	2017	Numerical	*HCT*	Water
Hardik and S.V. Prabhu [32]	2017	Experimental	*HCT*	Water
Wang et al. [33]	2018	Numerical	*HCT*	Water
Bhanvase et al. [34]	2018	Experimental	*HCT*	Water based PANI nanofluid
F. Li and B. Bai [35]	2018	Numerical	*HCT*	Supercritical Water
Khosravi-Bizhaem et al. [36]	2019	Experimental	*HCT*	Water
Wang et al. [37]	2019	Experimental and numerical	*HCT*	Water
Sheeba et al. [11]	2020	Experimental and numerical	*CCT*	Water
Abdelmagied [38]	2020	Experimental and numerical	*CCT*	Water
Li et al. [39]	2023	Numerical	*HCT*	Water
Present Study	2023	Experimental	*CCT*	Al_2O_3*/Water*

II. EXPERIMENTAL SETUP AND PROCEDURE

The experimental test rig is depicted in Figure 1. Conically coiled tubes (test section), storage tank, cooling system, pump, pipes, control system, flowmeter, and pressure sensors comprise the experimental setup. Table 2 shows the geometric parameters of the three *CCT*s with the same curvature ratio but different coil torsions. The nanofluid tank is filled with nanofluid with the required volume fraction of nanoparticles. The reservoir's external wall was covered to avoid losing heat and was made of stainless steel.

The thermocouples are first attached to the appropriate positions. Afterwards, nanofluid was cycled through into

DOI: 10.21608/ERJENG.2023.192940.1152

Journal of Engineering Research (ERJ)
Vol. 7 – No. 1, 2023
©Tanta University, Faculty of Engineering
ISSN: 2356-9441 https://erjeng.journals.ekb.eg/ e ISSN: 2735-4873

the test section (*CCT*) and the experiment was conducted with the proper equipment to regulate and measure the factors that affect the heat transfer and pressure drop. Included in these factors are flow rate, temperature, and pressure.

The instruments used in the experimental setting are detailed in Table 3. The uniform heat flux on the tubes' surfaces was provided using an electrical heater that was wound around a CCT and adequately insulated. Twelve K-type thermocouples were used to determine the surface temperatures of the tube, and all temperatures were collected using a data acquisition device. All parameters are collected and stored when the system enters a steady state.

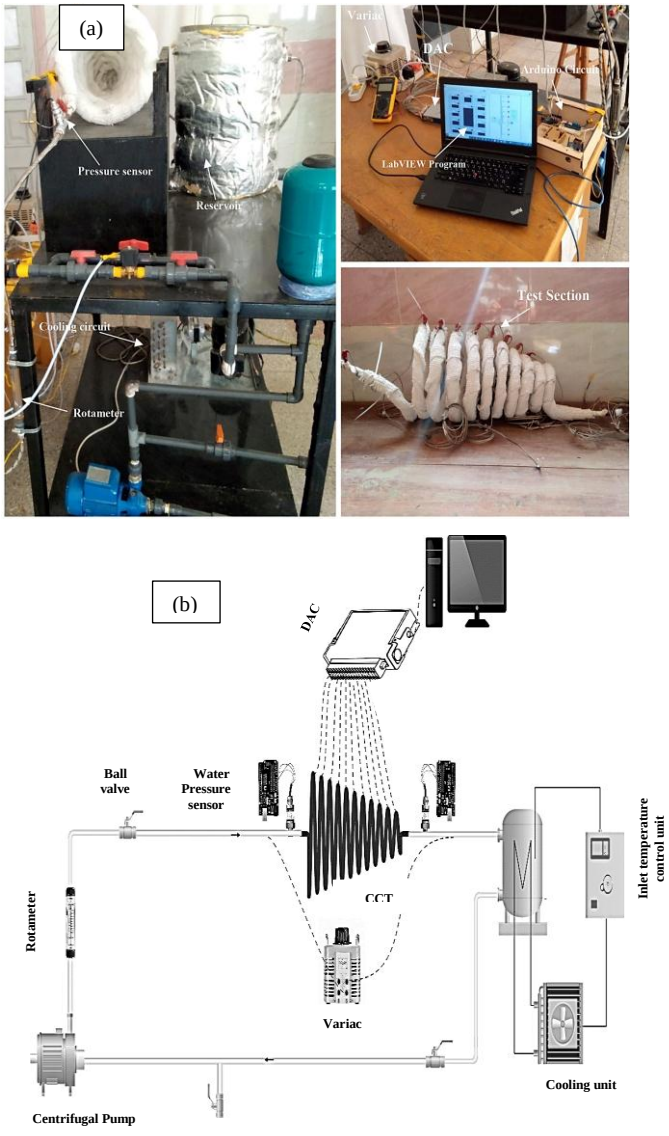

Fig. 1. Experimental setup, a) photograph view, and b) Schematic diagram.

Table 2. Current research geometrical parameters

Coil	Shape	Coil Torsion (λ)	Curvature Ratio (δ)	Coil Pitch	Cone Angle
Coil #1	*CCT*	*0.02*	*0.0564*	*12.7 mm*	*45°*
Coil #2	*CCT*	*0.036*	*0.0564*	*22.7 mm*	*45°*
Coil #3	*CCT*	*0.052*	*0.0564*	*32.7 mm*	*45°*

Table 3. Instrumental measuring device accuracy

Measured Parameter	Instrument	Accuracy /Uncertainty
Coil diameter	Vernier caliper	±0.01 mm
Pressure drop	Water pressure sensor; SKU: SEN0257	0.5%~1% F.S
Flow rate	Water flow sensor; YF-S201	±3%.
Temperature	K-type	± 1.5 ℃

III. PREPARATION AND STABILITY OF NANOFLUID

In this study, a stable Al_2O_3/water nanofluid was used as a heat transfer fluid. Al_2O_3 nanoparticles with a notional average diameter of 50 nm were suspended in distilled water using a two-step procedure. The nanofluid was created with three concentrations by volume: 0.3%, 0.6%, and 0.9%.

Utilizing the appropriate surfactants, nanoparticles are suspended in nanofluid, and an ultrasonic bath is then used to separate the nanofluid clusters. During a 6-day visual examination of the stability, no sedimentation was seen. As demonstrated in Fig. 2, the free surface did not appear until 7 days had passed. Table 4 shows the thermo-physical properties of pure water and Al_2O_3 nanoparticles. Fig. 3 shows *transmission electron microscopy (TEM)* analysis of Al_2O_3 nanoparticles to identify their size. The average size of nanoparticles is 50 nm.

After preparation **After 7 days**

Fig. 2. Nanofluid stability check.

Table 4. Thermo-physical properties of Pure water and Al2O3 nanoparticles at room temperature

Physical Properties	Pure Water	Al_2O_3 Nanoparticles
Cp (J/Kg.˚K)	4180	773
ρ (Kg/m^3)	998	3600
K (W/m.˚K)	0.607	36

DOI: 10.21608/ERJENG.2023.192940.1152

Journal of Engineering Research (ERJ)
Vol. 7 – No. 1, 2023
©Tanta University, Faculty of Engineering
ISSN: 2356-9441 https://erjeng.journals.ekb.eg/ e ISSN: 2735-4873

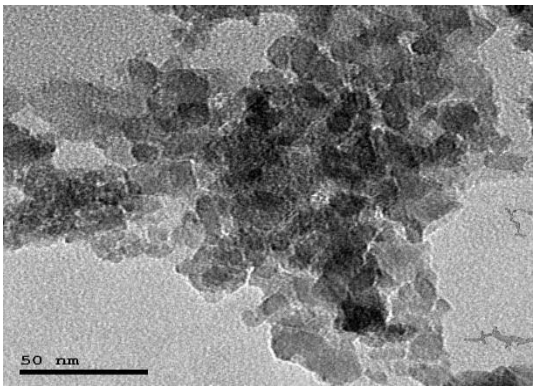

Fig. 3. TEM of Al_2O_3 nanoparticles

IV. DATA PROCESSING

A. Thermo-physical Properties of Nanofluid

Assuming that the nanoparticles are uniformly dispersed throughout the base fluid, the relevant physical properties of the composites have been computed via well formulas/models for single-phase fluids, as given in Table 5.

B. Heat Transfer Calculations

For the estimation of *Nu* and f, the bulk temperature of a fluid was determined using the following formula.

$$T_b = \frac{T_i + T_e}{2} \quad (11)$$

The following formula is used to calculate the total rate of heat transfer in the *CCT*s:

$$Q^{\circ} = \dot{m}\, C_p (T_e - T_i) \quad (12)$$

Because it was possible to measure the temperature at multiple sites along the tube, the heat transfer coefficient was computed locally in this study. The local h was computed as follows [27].

$$h_x = \frac{\dot{Q}}{A\,(T_{w,x} - T_{b,x})} \quad (13)$$

where $T_{w,x}$ is the wall surface temperature and $T_{b,x}$ is the fluid bulk temperature at each location.

$$T_{b,x} = T_i + \frac{\dot{q}\,P}{\dot{m}\,C_p} x, \qquad \dot{q} = \frac{\dot{Q}}{A} \quad (14)$$

Using the trapezoidal approach, the average h was calculated numerically by integrating the local values along the length of the tube as follows [28]:

$$h_{avg} = \frac{1}{L}\int_0^L h_{(x)}\, dx \quad (15)$$

Table 5. Standardized formulae for calculating the thermo-physical properties of nanofluids

Properties	Formula	Eq. No.
Density (ρ_{nf}) [23]	$\rho_{nf} = \varphi\,\rho_{np} + (1-\varphi)\,\rho_{bf}$	(1)
Specific heat ($C_{p,nf}$) [24]	$C_{p,nf} = \frac{\varphi\,(\rho_{np}\,C_{p,np}) + (1-\varphi)(\rho_{bf}\,C_{p,bf})}{\rho_{nf}}$	(2)
Thermal conductivity (k_{nf}) [25]	$k_{nf} = k_{static} + k_{brownian}$	(3)
	$K_{static} = K_{bf}\left[\frac{K_{np} + 2K_{bf} + 2\varphi\,(K_{np} - K_{bf})}{K_{np} + 2K_{bf} - \varphi\,(K_{np} - K_{bf})}\right]$	(4)
	$K_{brownian} = 5 * 10^4\,\beta\,\varphi\,\rho_{bf}\,c_{p,bf}\sqrt{\frac{\kappa_B\,T}{\rho_{np}\,d_{np}}}\,\Gamma(T,\varphi)$	(5)
	$\Gamma = (-134.63 + 1722.3\,\varphi) + (0.4705 - 6.04\,\varphi)T$	(6)
	$\beta = 0.0017(100\,\varphi)^{-0.0841}$	(7)
Viscosity (μ_{nf}) [25,26]	$\mu_{nf} = \mu_{static} + \mu_{brownian}$	(8)
	$\mu_{static} = \frac{1}{(1-\varphi)^{2.5}}\mu_{bf}$	(9)
	$\mu_{brownian} = 5 * 10^4\,\beta\,\varphi\,\rho_{bf}\sqrt{\frac{\kappa_B\,T}{\rho_{np}\,d_{np}}}$	(10)

DOI: 10.21608/ERJENG.2023.192940.1152

Journal of Engineering Research (ERJ)
Vol. 7 – No. 1, 2023
©Tanta University, Faculty of Engineering
ISSN: 2356-9441 https://erjeng.journals.ekb.eg/ e ISSN: 2735-4873

The following formulas were used to get the average *Nu* and *f*:

$$Nu_{avg} = \frac{h_{avg}\, d}{K} \quad (16)$$

$$f = \frac{\Delta P_c\, \pi^2\, \rho_t\, d_{t,i}^5}{32\, L_t\, \dot{m}_t^2} \quad (17)$$

V. UNCERTAINTY ANALYSIS

The accuracy of experimental results is contingent upon the accuracy of specific measuring devices and methodologies. Kline and McClintock [29] showed that a root-sum-square combination of the effects of the different inputs can be used to find the uncertainty in a calculated result with a high degree of accuracy.The partial derivatives of each variable are assessed in order to weight the overall uncertainty based on the uncertainty associated with each variable. The major parameters, h_{avg} and f, employed in this work to interpret experimental results are dependent of several factors, including laboratory measurement data and physical attributes. The uncertainty of the preceding experiment was evaluated using Equation (18).

$$R = R(x_1, x_2, \dots\dots, x_J) \qquad U_R = \sqrt{\sum_{i=1}^{J} \left(\frac{\partial R}{\partial X_i} U_i\right)^2} \quad (18)$$

R is a function of J independent measurable variables. U_R and U_i are the result and independent variable measurement uncertainties, respectively. Table 6 summarises, for all experimental runs, the average uncertainty of key parameters.

VI. RESULTS AND DISCUSSION

In this section, the major outcomes of the experimental testing for water and *Al_2O_3/water* are presented and described in depth. Experiments were performed on *CCT*s with *De* ranging from 1148 to 2983, concentrations of nanoparticles varying from 0.3% to 0.9%, and λ ranging between 0.02 and 0.052 using the same curvature ratio. The flow rate ranged from 0.03 to 0.09 kg/s, and the fluid temperature at the entry of the *CCT*s was kept at 25 °C.

A. Heat Transfer Results

According to earlier research [7, 8, 12], the addition of nanoparticles to pure water enhances the thermal conductivity and, therefore, the *HTR*s. Increasing the volume concentration of *Al_2O_3* nanoparticles will further enhance heat conductivity and the disruptive effect of the nanoparticles. Figure 4 illustrates the variation in h_{avg} versus *De*. A decrease in the coil's torsion led to an increase in h_{avg}, according to the results. This is a consequence of the amplification and expansion of secondary flow, which leads to enhanced *HTR*. *CCT*s produce secondary flow generation to facilitate the mixing of nanoparticles with low-viscosity fluids while preserving the nanofluids' stability.

Table 6. Average uncertainties of the most important parameters.

Parameter	Average Uncertainty (%)
Dean Number (*De*)	±1.9
Average heat transfer coefficient (h_{avg})	±4.8
Fanning friction factor (*f*)	±4.1

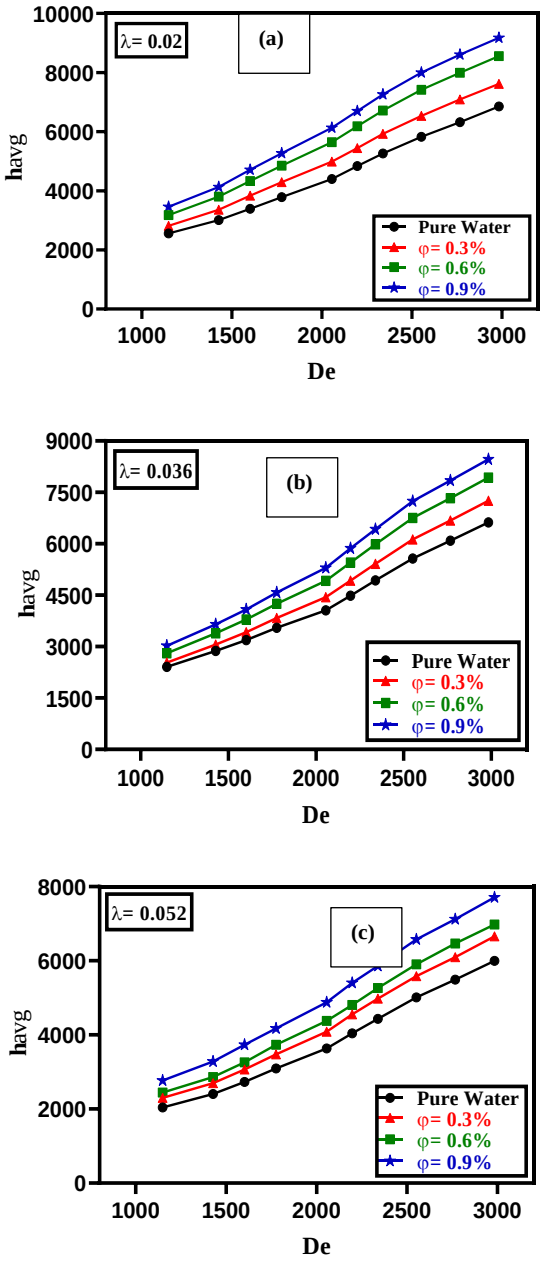

Fig. 4. Variation of average h with Dean number for (a) λ= 0.02, (b) λ= 0.036 and (c) λ= 0.052.

DOI: 10.21608/ERJENG.2023.192940.1152

Journal of Engineering Research (ERJ)
Vol. 7 – No. 1, 2023
©Tanta University, Faculty of Engineering
https://erjeng.journals.ekb.eg/
ISSN: 2356-9441
e ISSN: 2735-4873

In addition, according to the data, boosting the Al_2O_3/water nanofluid concentration from 0.3% to 0.9% increased h_{avg}. The average increase in h_{avg} at lower and higher *De* values is 32% and 26%, respectively. The incorporation of nanoparticles may improve the *HTR* owing to the higher thermal conductivity of Al_2O_3/water nanofluid as well as the randomized motion of nanoparticles, which promotes heat transfer. In other words, the processes of heat transmission get more intense as the concentration of nanoparticles increases.

Figure 5 depicts the experimental average h of *Al_2O_3/water* nanofluid to that of pure water $\left(\frac{h_{nf}}{h_w}\right)$ within *CCT*s at all nanofluid concentrations tested. As predicted, this ratio rises with increasing volume fraction of nanoparticles. For instance, the ratio of the average h of nanofluids to that of distilled water ranges between 1.28 and 1.5 for 0.9% nanofluids within *CCT*s.

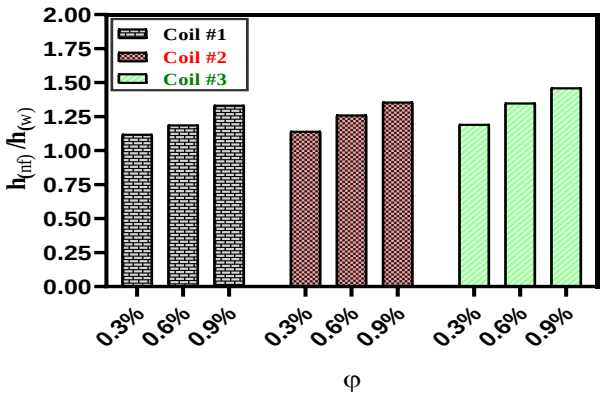

Fig. 5. The variations of relative h_{avg} with ϕ at different coil torsions

B. Pressure Drop Results

The hydraulic performance may be evaluated by measuring the pressure drop over the investigated CCTs. Three volume concentrations of Al_2O_3 nanoparticles are considered: 0.3%, 0.6%, and 0.9% at coil torsion (λ) varied from 0.02 to 0.052. *The* relationship between friction factor (f) and *De* is shown in Fig. 6.

The friction factor (f) tends to decrease as *De* increases. This is brought on by an increase in centrifugal force and the consequent formation of vortices brought on by a reduction in torsion or rotational impact. According to the data, increasing the Al_2O_3/water nanofluid's concentration from 0.3% to 0.9% also decreased f. For low *De* and high *De*, respectively, the average increment in f is 40% and 22%. When nanoparticles are included, the *HTR* may be increased due to the greater thermal conductivity of nanofluid and the randomized motion of nanoparticles, both of which contribute to enhancing heat transfer. Furthermore, the dynamic viscosity has a significant impact on the drop in pressure across the *CCT*s, rather than the nanoparticles' density, velocity, and concentration. This impact increases significantly with increasing nanoparticle concentration [30].

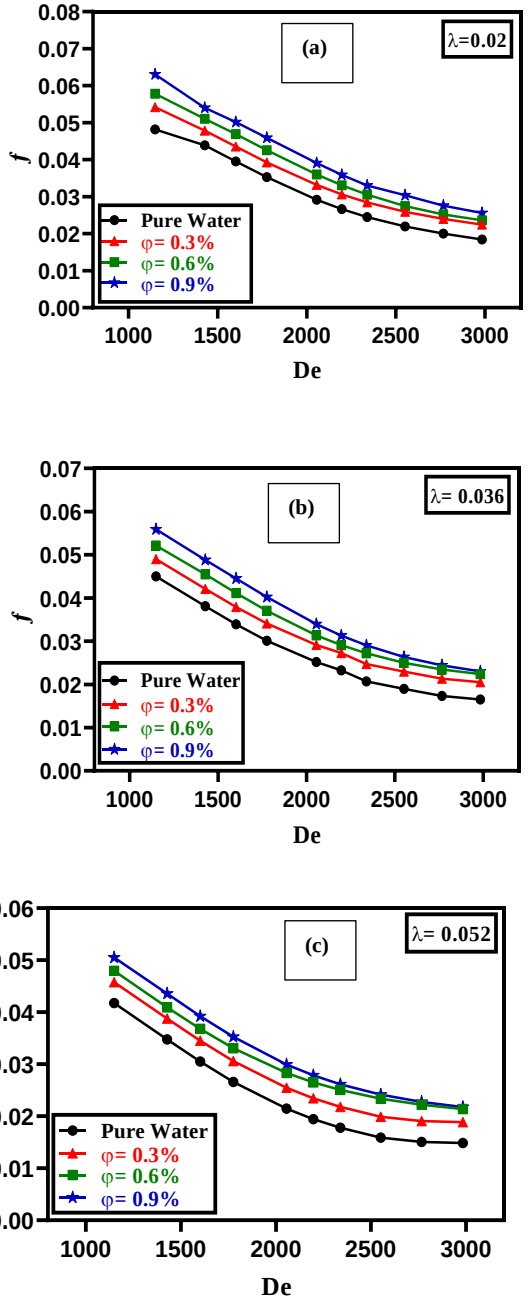

Fig. 6. Variation of f with Dean number for (a) λ= 0.02, (b) λ= 0.036 and (c) λ= 0.052.

C. Thermal-Hydraulic Performance

The thermal performance factor (*TPF*) is situated between the augmentation of heat transfer and the pressure drop of the *CCT*s. It is used to evaluate the heat transfer improvement of *CCT*s under the same pumping power and may be computed using the following formula:

DOI: 10.21608/ERJENG.2023.192940.1152

Journal of Engineering Research (ERJ)
Vol. 7 – No. 1, 2023
©Tanta University, Faculty of Engineering
ISSN: 2356-9441 https://erjeng.journals.ekb.eg/ e ISSN: 2735-4873

$$TPF = \frac{\left(\frac{Nu_{nf}}{Nu_w}\right)}{\left(\frac{f_{nf}}{f_w}\right)^{\frac{1}{3}}} \quad (19)$$

In this study, the *TPF* is utilized to assess the performance of *CCT*s using *Al_2O_3/water* nanofluid and compared to the comparable value for pure water. The average *h* and *f* are insufficient only for determining the performance *CCT*s. Consequently, the thermal performance factor is shown in this section to demonstrate the superior performance of *CCT*s.

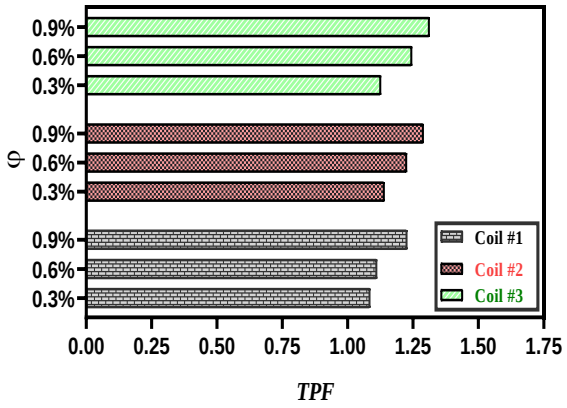

Fig. 7. The variations of TPF with ϕ at different coil torsions

The relationship between the *TPF* and φ for varying particle volume fractions is depicted in Fig. 7. In general, the *TPF* increases with increasing *Al_2O_3/water* nanofluid nanoparticle concentrations. It indicates that in all conditions under consideration, heat gain exceeds pressure loss. The capacity of the nanopowder to increase the thermal conductivity of the base fluid is given as the first explanation, while the mobility of nanoparticles allowing energy transfer is proposed as the second explanation.

According to Fig. 7, *TPF* values larger than unity show that the heat transfer augmentation process exceeds the pressure drop penalty advance, demonstrating the efficiency of *CCT*s and nanofluids in enhancing system performance. The *TPF* increased by 26% when the φ was increased from 0.3% to 0.9% for coil #1 with the same De value. For coil #2, the *TPF* increased by 22%. Furthermore, for coil #3, the *TPF* increased by 19%.

VII. CONCLUSIONS

This work was conducted to investigate the effects of Al_2O_3/water *nanofluid* on the pressure drop and heat transfer of conically coiled tubes (*CCT*s). The thermo-hydraulic properties of *CCT*s with Dean numbers (*De*) ranging from 1148 to 2983, coil torsions ranging from 0.02 to 0.052, and particle volume concentration values ranging from 0.3% to 0.9% were investigated. In addition to that, the outcomes that were achieved are as follows:

- A reduction in *CCT*'s coil torsion resulted in an increase in the average heat transfer coefficient. This is related to the development and enhancement of secondary flow, which contributes to the improvement of heat transfer rates.
- The average heat transfer coefficient increased as the nanofluid concentration went from 0.3% to 0.9%. The average increase is 32% at lower values of *De* and 26% at higher values of *De*. Due to their higher thermal conductivity and the random motion of the nanoparticles, *Al_2O_3/water* nanofluids are better at transferring heat than pure water.
- The Dean number has a tendency to increase, which results in a reduction in the friction factor.
- The thermal performance factor (*TPF*) increased when the coil torsion decreased from 0.052 to 0.02. Due to the fact that the *TPF* for testing nanofluids is more than unity, the employment of nanofluids and *CCT*s is an energy-efficient way for increasing the thermal capacity of equipment.

VIII. FUTURE RECOMMANDATIONS

Hyper nanofluids may be used to conduct future studies in this area. In addition, the geometry of the coil may be altered in conjunction with a thorough examination of other operating conditions. A numerical model may also be used, and its results may be compared to the experimental findings of this study. The use of nanofluids has become an urgent need to improve the heat transfer process of thermal equipment, particularly those that operate at high temperatures under complex working conditions.

Funding: This research has not received any type offunding.

Conflicts of Interest: The authors declare that there is noconflict of interest.

NOMENCLATURES

Symbols	Definition
A	Area
C_p	Specific heat
d	Diameter
h	convection heat transfer coefficient
K	Thermal conductivity
L	Length
m	Mass
ṁ	Mass flow rate
P_c	Pitch
P	perimeter of tube
Q˚	Rate of heat transfer
q˚	Heat flux
S	Spacing of coiled tube
T	Temperature

DOI: 10.21608/ERJENG.2023.192940.1152

Journal of Engineering Research (ERJ)
Vol. 7 – No. 1, 2023
©Tanta University, Faculty of Engineering
ISSN: 2356-9441 https://erjeng.journals.ekb.eg/ e ISSN: 2735-4873

x	distance

Subscript

avg	average
b	Bulk
bf	Base fluid
c	coil
e	exit
i	inlet
L	large
nf	Nanofluid
np	Nanoparticle
s	small
t	tube
w	Wall or Water
x	Local variable

GREEK LETTERS

Letters	Definition
δ	Coil curvature ratio, $d_{t,i}/D_c$
λ	Coil torsion, $P_c/\pi D_c$
π	Pi ≡ A mathematical constant ≅ 3.1416
ρ	Density (kg/m)
Γ	Modelling function
κ	Boltzmann constant, $1.3807 * 10^{-23}$ (J/K)
μ	Dynamic viscosity (kg/m.s)
φ	Particles volume concentration
β	Interaction between fluid particles and nanoparticles
f	Friction factor

DIMENSIONLESS GROUPS

Symbols	Definition
De	Dean number, $D_e = Re\sqrt{\delta}$
Nu	Nusselt number
Re	Reynolds number

ABBREVIATIONS

Abbreviations	Definition
Ag	Silver
Al_2O_3	Aluminum Oxide
CCT	Conically Coiled Tube
CuO	Copper oxide
EG	Ethylene glycol
GO	Graphene Oxide
HCT	Helically Coiled Tube
HTR	Heat Transfer Rate
MWCNT	Multi-walled Carbon Nanotubes
ND	Nanodiamond
SiO_2	Silicon dioxide
TiO_2	Titanium dioxide
TPF	Thermal performance factor

REFERENCES

1] E.A. Chavez Panduro, F. Finotti, G. Largiller, K.Y. Lervag, A review of the use of nanofluids as heat-transfer fluids in parabolic-trough collectors, Appl. Therm. Eng. 211 (2022) 118346. https://doi.org/10.1016/j.applthermaleng.2022.118346.
[2] W. Ajeeb, S.M.S. Murshed, Nanofluids in compact heat exchangers for thermal applications: A State-of-the-art review, Therm. Sci. Eng. Prog. 30 (2022) 101276. https://doi.org/10.1016/j.tsep.2022.101276.
[3] Z. Islam, A.K. Azad, M.J. Hasan, R. Hossain, M.M. Rahman, Unsteady periodic natural convection in a triangular enclosure heated sinusoidally from the bottom using CNT-water nanofluid, Results Eng. 14 (2022) 100376. https://doi.org/10.1016/j.rineng.2022.100376.
[4] M.J. Hasan, A.K. Azad, Z. Islam, R. Hossain, M.M. Rahman, Periodic Unsteady Natural Convection on CNT Nano-powder Liquid in a Triangular Shaped Mechanical Chamber, Int. J. Thermofluids. 15 (2022) 100181. https://doi.org/10.1016/j.ijft.2022.100181.
[5] R. Hossain, M.J. Hasan, A.K. Azad, M.M. Rahman, Numerical study of low Reynolds number effect on MHD mixed convection using CNT-oil nanofluid with radiation, Results Eng. 14 (2022) 100446. https://doi.org/10.1016/j.rineng.2022.100446.
[6] E.I. Jassim, F. Ahmed, Assessment of nanofluid on the performance and energy-environment interaction of Plate-Type-Heat exchanger, Therm. Sci. Eng. Prog. 25 (2021) 100988. https://doi.org/10.1016/j.tsep.2021.100988.
[7] A.H. Rasheed, H.B. Alias, S.D. Salman, Experimental and numerical investigations of heat transfer enhancement in shell and helically microtube heat exchanger using nanofluids, Int. J. Therm. Sci. 159 (2021) 106547. https://doi.org/10.1016/j.ijthermalsci.2020.106547.
[8] H.M. Maghrabie, M. Attalla, A. A. A. Mohsen, Performance assessment of a shell and helically coiled tube heat exchanger with variable orientations utilizing different nanofluids, Appl. Therm. Eng. 182 (2021) 116013. https://doi.org/https://doi.org/10.1016/j.applthermaleng.2020.116013.
[9] S.M. Elshamy, M.T. Abdelghany, M.R. Salem, O.E. Abdellatif, Energy and exergy analysis of shell and coil heat exchanger using water based Al_2O_3 nanofluid including diverse coil geometries: An experimental study, J. Nanofluids. 9 (2020) 13–23. https://doi.org/10.1166/JON.2020.1727.
[10] M.M. Heyhat, A. Jafarzad, P. Changizi, H. Asgari, M. Valizade, Experimental research on the performance of nanofluid flow through conically coiled tubes, Powder Technol. 370 (2020) 268–277. https://doi.org/10.1016/j.powtec.2020.05.058.
[11] A. Sheeba, R. Akhil, M.J. Prakash, Heat transfer and flow characteristics of a conical coil heat exchanger, Int. J. Refrig. 110 (2020) 268–276. https://doi.org/10.1016/j.ijrefrig.2019.10.006.
[12] M. Mansouri, S.A.H. Zamzamian, Experimental studies on the heat transfer characteristics of alumina/water nanofluid inside a helical coil tube, Heat Mass Transf. 57 (2021) 551–564. https://doi.org/10.1007/s00231-020-02976-w.
[13] M.J. Hasan, A.A. Bhuiyan, Investigation of thermal performance and entropy generation in a helical heat exchanger with multiple rib profiles

Journal of Engineering Research (ERJ)
Vol. 7 – No. 1, 2023
©Tanta University, Faculty of Engineering
ISSN: 2356-9441 https://erjeng.journals.ekb.eg/ e ISSN: 2735-4873

using Al_2O_3-water nanofluid, Case Stud. Therm. Eng. 40 (2022) 102514. https://doi.org/10.1016/j.csite.2022.102514.
[14] L.S. Sundar, F. Shaik, Heat transfer and exergy efficiency analysis of 60% water and 40% ethylene glycol mixture diamond nanofluids flow through a shell and helical coil heat exchanger, Int. J. Therm. Sci. 184 (2023) 107901. https://doi.org/10.1016/j.ijthermalsci.2022.107901.
[15] M.J. Hasan, S.F. Ahmed, A.A. Bhuiyan, Geometrical and coil revolution effects on the performance enhancement of a helical heat exchanger using nanofluids, Case Stud. Therm. Eng. 35 (2022) 102106. https://doi.org/10.1016/j.csite.2022.102106.
[16] S. Kia, S. Khanmohammadi, A. Jahangiri, Experimental and numerical investigation on heat transfer and pressure drop of SiO_2 and Al_2O_3 oil-based nanofluid characteristics through the different helical tubes under constant heat fluxes, Int. J. Therm. Sci. 185 (2023) 108082. https://doi.org/10.1016/j.ijthermalsci.2022.108082.
[17] A. Güngör, A. Khanlari, A. Sözen, H.I. Variyenli, Numerical and experimental study on thermal performance of a novel shell and helically coiled tube heat exchanger design with integrated rings and discs, Int. J. Therm. Sci. 182 (2022). https://doi.org/10.1016/j.ijthermalsci.2022.107781.
[18] S. Fuxi, N. Sina, A. Ahmadi, E.H. Malekshah, M.Z. Mahmoud, H. Aybar, Effect of different pitches on the 3D helically coiled shell and tube heat exchanger filled with a hybrid nanofluid: Numerical study and artificial neural network modeling, Eng. Anal. Bound. Elem. 143 (2022) 755–768. https://doi.org/10.1016/j.enganabound.2022.07.018.
[19] A.D. Tuncer, A. Khanlari, A. Sözen, E.Y. Gürbüz, H.İ. Variyenli, Upgrading the performance of shell and helically coiled heat exchangers with new flow path by using TiO2/water and CuO–TiO_2/water nanofluids, Int. J. Therm. Sci. 183 (2022). https://doi.org/10.1016/j.ijthermalsci.2022.107831.
[20] P.C. Mukesh Kumar, M. Chandrasekar, Heat transfer and friction factor analysis of MWCNT nanofluids in double helically coiled tube heat exchanger, J. Therm. Anal. Calorim. 144 (2021) 219–231. https://doi.org/10.1007/s10973-020-09444-x.
[21] A.H. Al-Abbas, A.A. Mohammed, A.S. Hassoon, Exergy analysis of Shell and helical coil heat exchanger and design optimization, Heat Mass Transf. 57 (2021) 797–806. https://doi.org/10.1007/s00231-020-02993-9.
[22] M. Basit Shafiq, U. Allauddin, M.A. Qaisrani, T. ur Rehman, N. Ahmed, M. Usman Mushtaq, H.M. Ali, Thermal performance enhancement of shell and helical coil heat exchanger using MWCNTs/water nanofluid, J. Therm. Anal. Calorim. 147 (2022) 12111–12126. https://doi.org/10.1007/s10973-022-11405-5.
[23] B.C. Pak, Y.I. Cho, Hydrodynamic And Heat Transfer Study Of Dispersed Fluids With Submicron Metallic Oxide Particles, Exp. Heat Transf. 11 (1998) 151–170. https://doi.org/10.1080/08916159808946559.
[24] Y. Xuan, W. Roetzel, Conceptions for heat transfer correlation of nanofluids, Int. J. Heat Mass Transf. 43 (2000) 3701–3707. https://doi.org/https://doi.org/10.1016/S0017-9310(99)00369-5.
[25] J. Koo, C. Kleinstreuer, A new thermal conductivity model for nanofluids, J. Nanoparticle Res. 6 (2004) 577–588. https://doi.org/10.1007/s11051-004-3170-5.
[26] H.C. Brinkman, The Viscosity of Concentrated Suspensions and Solutions, Jcp. 20 (1952) 571. https://doi.org/10.1063/1.1700493.
[27] F. Incropera, D. Dewitt, T. Bergman, Fundamentals of heat and mass transfer, 2011.
[28] M. Gilli, D. Maringer, E. Schumann, Numerical methods and optimization in finance, Numer. Methods Optim. Financ. (2019) 1–614. https://doi.org/10.1016/C2017-0-01621-X.
[29] Kline SJ, McClintock F, Describing uncertainty in single sample experiments, Mech Eng. 57 (1953) 3–8.
[30] S. Mirfendereski, A. Abbassi, M. Saffar-Avval, Experimental and numerical investigation of nanofluid heat transfer in helically coiled tubes at constant wall heat flux, Adv. Powder Technol. 26 (2015) 1483–1494. https://doi.org/10.1016/j.apt.2015.08.006.
[31] A. Alimoradi, M. Olfati, M. Maghareh, Numerical investigation of heat transfer intensification in shell and helically coiled finned tube heat exchangers and design optimization, Chem. Eng. Process. Process Intensif. 121 (2017) 125–143. https://doi.org/10.1016/j.cep.2017.08.005.
[32] B.K. Hardik, S. V Prabhu, Critical heat flux in helical coils at low pressure, Appl. Therm. Eng. 112 (2017) 1223–1239. https://doi.org/https://doi.org/10.1016/j.applthermaleng.2016.10.114.
[33] J. Wang, S.S. Hashemi, S. Alahgholi, M. Mehri, M. Safarzadeh, A. Alimoradi, Analysis of Exergy and energy in shell and helically coiled finned tube heat exchangers and design optimization, Int. J. Refrig. 94 (2018) 11–23. https://doi.org/10.1016/j.ijrefrig.2018.07.028.
[34] B.A. Bhanvase, S.D. Sayankar, A. Kapre, P.J. Fule, S.H. Sonawane, Experimental investigation on intensified convective heat transfer coefficient of water based PANI nanofluid in vertical helical coiled heat exchanger, Appl. Therm. Eng. 128 (2018) 134–140. https://doi.org/https://doi.org/10.1016/j.applthermaleng.2017.09.009.
[35] F. Li, B. Bai, Flow and heat transfer of supercritical water in the vertical helically-coiled tube under half-side heating condition, Appl. Therm. Eng. 133 (2018) 512–519. https://doi.org/https://doi.org/10.1016/j.applthermaleng.2018.01.047.
[36] H. Khosravi-Bizhaem, A. Abbassi, A. Zivari Ravan, Heat transfer enhancement and pressure drop by pulsating flow through helically coiled tube: An experimental study, Appl. Therm. Eng. 160 (2019) 114012. https://doi.org/10.1016/j.applthermaleng.2019.114012.
[37] G. Wang, D. Wang, X. Peng, L. Han, S. Xiang, F. Ma, Experimental and numerical study on heat transfer and flow characteristics in the shell side of helically coiled trilobal tube heat exchanger, Appl. Therm. Eng. 149 (2019) 772–787. https://doi.org/10.1016/j.applthermaleng.2018.11.055.
[38] M.M. Abdelmagied, Investigation of the triple conically tube thermal performance characteristics, Int. Commun. Heat Mass Transf. 119 (2020) 104981. https://doi.org/10.1016/j.icheatmasstransfer.2020.104981.
[39] Y. Li, Q. Yu, S. Yu, P. Zhang, J. Zhang, Numerical investigation and mechanism analysis of heat transfer enhancement in a helical tube by square wave pulsating flow, Heat Mass Transf. (2023) 21–37. https://doi.org/10.1007/s00231-022-03231-0.
[40] A. Khalil, S. El-Agouz, A. Zohir, A. Farid, Performance Enhancement of Double Tube Heat Exchanger Using Coiled Fins, J. Eng. Res. 3 (2019) 41–49. https://doi.org/10.21608/erjeng.2019.125492.
[41] H. Khosravi-Bizhaem, A. Abbassi, M.R. Salimpour, A. Zivari-Ravan, Experimental study on heat transfer, entropy generation, and exergy destruction of Ag, MWCNT, and GO water-based nanofluids in helical tubes, J. Therm. Anal. Calorim. 147 (2022) 2761–2784. https://doi.org/10.1007/s10973-021-10655-z.

DOI: 10.21608/ERJENG.2023.192940.1152